

# Topological and Functional Relationship of Subunits $F_1$ - $\gamma$ and $F_0$ I-PVP(b) in the Mitochondrial $H^+$ -ATP Synthase<sup>†</sup>

Antonio Gaballo, Franco Zanotti, Angela Solimeo, and Sergio Papa\*

*Institute of Medical Biochemistry and Chemistry, University of Bari, Bari, Italy*

*Received June 16, 1998; Revised Manuscript Received August 14, 1998*

**ABSTRACT:** Diamide treatment of the  $F_0F_1$ -ATP synthase in “inside out” submitochondrial particles (ESMP) in the absence of a respiratory  $\Delta\mu H^+$  as well as of isolated  $F_0$  reconstituted with  $F_1$  or  $F_1$ - $\gamma$  subunit results in direct disulfide cross-linking between cysteine 197 in the carboxy-terminal region of the  $F_0$ I-PVP(b) subunit and cysteine 91 at the carboxyl end of a small  $\alpha$ -helix of subunit  $F_1$ - $\gamma$ , both located in the stalk. The  $F_0$ I-PVP(b) and  $F_1$ - $\gamma$  cross-linking cause dramatic enhancement of oligomycin-sensitive decay of  $\Delta\mu H^+$ . In ESMP and MgATP particles the cross-linking is accompanied by decoupling of respiratory ATP synthesis. These effects are consistent with the view that  $F_0$ I-PVP(b) and  $F_1$ - $\gamma$  are components of the stator and rotor of the proposed rotary motor, respectively. The fact that the carboxy-terminal region of  $F_0$ I-PVP(b) and the short  $\alpha$ -helix of  $F_1$ - $\gamma$  can form a direct disulfide bridge shows that these two protein domains are, at least in the resting state of the enzyme, in direct contact. In isolated  $F_0$ , diamide also induces cross-linking of OSCP with another subunit of  $F_0$ , but this has no significant effect on proton conduction. When ESMP are treated with diamide in the presence of  $\Delta\mu H^+$  generated by respiration, neither cross-linking between  $F_0$ I-PVP(b) and  $F_1$ - $\gamma$  subunits nor the associated effects on proton conduction and ATP synthesis is observed. Cross-linking is restored in respiring ESMP by  $\Delta\mu H^+$  collapsing agents as well as by DCCD or oligomycin. These observations indicate that the torque generated by  $\Delta\mu H^+$  decay through  $F_0$  induces a relative motion and/or a separation of the  $F_0$ I-PVP(b) subunit and  $F_1$ - $\gamma$  which places the single cysteine residues, present in each of the two subunits, at a distance at which they cannot be engaged in disulfide bridging.

The ATP synthase<sup>1</sup> of coupling membranes consists of a globular catalytic moiety,  $F_1$ ,<sup>2</sup> which protrudes out of the inner side of the membrane, a membrane integral proton translocating moiety,  $F_0$ , and a stalk which provides a structural and functional connection between  $F_1$  and  $F_0$  (1–4).

The X-ray crystallographic analysis of the structure of the bovine mitochondrial  $F_1$ -ATPase (5) has provided a structural basis for the binding change, rotatory mechanism of the catalytic process in  $F_1$ , in which the  $F_1$ - $\gamma$  subunit rotates in the central cavity of the  $F_1$ - $\alpha\beta\beta$  hexamer (6). Biochemical (7) and physical (8, 9) evidence for a rotatory movement of the  $F_1$ - $\gamma$  subunit relative to the  $\alpha\beta\beta$  hexamer has been obtained. The structural organization and the mechanism

of the proton translocating  $F_0$  sector (10–12), the mechanism by which the energy provided by transmembrane proton translocation through the  $F_0$  sector is transferred to  $F_1$  to drive ATP synthesis, and how the reverse process, that is, ATP-driven uphill proton translocation, occurs are less understood. The solution of these problems, and in particular that of energy coupling in the ATP synthase, rests on the elucidation of the structural and functional organization of the components of the stalk.

The stalk is made up of interdigitated extensions of  $F_1$  and  $F_0$  subunits which ensure transmission of the energy provided by a downhill flow of protons through the  $F_0$  domain in the membrane to the extrinsic  $F_1$  domain where ATP is synthesized from ADP and Pi. The crystal structure of bovine mitochondrial  $F_1$ -ATPase shows a stem protruding about 40 Å from the center of the bottom of the spherical body. This consists of the extension of the C-terminal and N-terminal  $\alpha$ -helices of the  $F_1$ - $\gamma$  subunit which runs in the central cavity of the  $\alpha\beta\beta$  hexamer. In the stem a third short  $\alpha$ -helix, residues 73–90, of the  $F_1$ - $\gamma$  subunit is identified. Cross-linking and mutational analysis show that in the *Escherichia coli*  $F_0F_1$  complex the  $\epsilon$  subunit (equivalent to the  $\delta$  subunit of the mitochondrial  $F_1$ ) is located in the stalk (13, 14). The crystal structure of the mitochondrial  $F_1$  shows, at the bottom of the sphere, that the stem is surrounded by alternating bundles of C-terminal  $\alpha$ -helices of the 3  $\alpha$  and 3  $\beta$  subunits. These are reached by  $F_0$  subunits contributing to the stalk, in which the central parts of the  $F_1$ - $\gamma$  subunit

<sup>†</sup> This work was financially supported by Grants No. 97.01167.PF49 Biotechnology Project, Consiglio Nazionale delle Ricerche, Italy, and the National Project of Murst for Bioenergetics and Membrane Transport, Italy.

<sup>1</sup> Enzymes: ATP synthase (EC 3.6.1.34); glucose-6-phosphate dehydrogenase (EC 1.1.1.49); catalase (EC 1.11.1.6); hexokinase (EC 2.7.1.1.).

<sup>2</sup> Abbreviations: FCCP, carbonylcyanide *p*-(trifluoromethoxy)phenylhydrazone; Chaps, 3-[(3-cholamidopropyl) dimethylammonio]-1-propanesulfonate; DCCD, *N,N'*-dicyclohexylcarbodiimide; DTT, dithiothreitol; SDS, sodium dodecyl sulfate; ESMP, submitochondrial particles prepared in the presence of EDTA; MgATP-SMP, submitochondrial particles prepared in the presence of Mg-ATP;  $F_0$ , membrane integral sector of  $H^+$ -ATP synthase;  $F_1$ , catalytic sector of bovine heart  $H^+$ -ATP synthase;  $F_1$ - $\gamma$ , protein subunit of mitochondrial  $F_1$ ;  $F_0$ I-PVP-(b), protein subunit of mitochondrial  $F_0$ ; OSCP, oligomycin-sensitivity conferring protein.

and the  $\epsilon$  subunit (in the *E. coli* enzyme) penetrate for most of its length (14).

In prokaryotic and eukaryotic ATP synthases  $F_0$  has three, conserved membrane intrinsic subunits:  $a$  and  $c$  which are essential for proton transport (11, 15), and the  $b$  subunit in *E. coli*, which is the least conserved component and has counterpart(s) in the eukaryotic enzymes (16–19). The bovine mitochondrial  $F_0$  has seven additional constituents, that is, subunits OSCP,  $d$ ,  $e$ ,  $f$ ,  $g$ ,  $F_6$ , and  $A_6L$  (20, 21). The  $F_0$  subunits contributing to the stalk in the mitochondrial ATP synthase have been identified with different approaches: (i) limited proteolysis of  $F_0$  and  $F_1$  subunits (16, 17, 22–24); (ii) immunodetection by subunit specific antibodies raised against purified  $F_0$  subunits (21, 23, 25); (iii) cross-linking of  $F_0$  and  $F_1$  subunits (25–30); and (iv) reconstitution from isolated subunits (31). Taken together, the results of these studies indicate that the carboxy-terminal region of  $F_0I$ -PVP( $b$ ) subunit, OSCP,  $F_6$ , and subunit  $d$  contribute to the stalk in the mitochondrial  $F_0F_1$ -ATP synthase. It is thought that OSCP (equivalent to subunit  $\delta$  of the *E. coli* enzyme) and  $F_0I$ -PVP( $b$ ) subunit are part, together with subunit  $a$  (ATPase 6), of the stator of the rotary motor, which holds the  $\alpha_3\beta_3$  hexamer, while the  $\gamma$  and  $\delta$  ( $\epsilon$  in *E. coli*) constitute, together with the multiple copies of the  $F_0$ - $c$  subunit, the rotor portion (7, 8, 32, 33). In this paper a study based on disulfide cross-linking is presented of the topological relationship of the  $F_1$ - $\gamma$  and  $F_0I$ -PVP( $b$ ) subunits in the stalk of the mitochondrial  $F_0F_1$ -ATP synthase and their functional interaction in the energy-linked  $H^+$  translocation. It should be noted that cysteine residues in mitochondrial  $F_0F_1$  subunits are very limited in number: C201 and C251 in  $F_1$ - $\alpha$ , C91 in  $F_1$ - $\gamma$ , C18 in  $F_1$ - $\epsilon$ , C197 in  $F_0I$ -PVP( $b$ ), C118 in OSCP, C100 in  $d$ , C72 in  $f$ , and C64 in  $c$  (4).

The present results provide evidence showing that the  $F_1$ - $\gamma$  and  $F_0I$ -PVP( $b$ ) subunits, components of the rotor and stator of the ATP synthase, respectively, are in direct contact and can form a disulfide bridge in the resting state of the enzyme. The respiratory  $\Delta\mu H^+$  induces a relative motion and/or separation of the two subunits at a distance which prevents their disulfide cross-linking.

## MATERIALS AND METHODS

Chemicals were purchased from the following companies: valinomycin, oligomycin, antimycin, nigericin, carbonylcyanide  $p$ -(trifluoromethoxy)phenylhydrazone (FCCP), diamide, and Chaps from Sigma Chemical Co.;  $N,N'$ -dicyclohexylcarbodiimide (DCCD) from Fluka;  $^{14}C$ -DCCD (50Ci/mol) from Amersham; acrylamide,  $N,N'$ -methylenebisacrylamide, sodium dodecyl sulfate (SDS), goat anti (rabbit IgG)-alkaline-phosphatase conjugate, and AP color development reagent (BCIP-5 bromo-4-chloro-3 indolyl phosphate) (NBT-nitroblue tetrazolium) from Bio-Rad; catalase from Boehringer; and nitrocellulose membrane (0.45  $\mu$ m pore size) from Schleicher and Schüll, Biotech, Ltd. All other chemicals were of high-purity grade.

**Preparations.** Inverted vesicles of the inner mitochondrial membrane were obtained by exposure of isolated beef heart mitochondria (34) to ultrasonic energy in the presence of EDTA at pH 8.5 (ESMP) or in the presence of 1 mM MgATP (MgATP-SMP) (35). Sequential treatment of ESMP with Sephadex chromatography (the  $F_1$  inhibitor protein was

removed) and urea (36) produced particles from which  $F_1$  subunits were removed (USMP). The percentage of inversion of submitochondrial particles was found to range from preparation to preparation from 96% to 100% (37).  $F_0$  sector was isolated by Chaps solubilization from USMP (38).  $F_1$  was purified by a modified (38) chloroform extraction procedure (39). The subunits  $F_1$ - $\alpha/\beta$  and  $\gamma$ ,  $F_0I$ -PVP( $b$ ) and OSCP were isolated by electroelution from preparative gel electrophoresis (40). After purification, all proteins were solubilized in 50 mM Tris/HCl, pH 7.4, 0.01% SDS (w/v), 50% glycerol (v/v) at a protein concentration of approximately 0.5  $\mu$ g/ $\mu$ L.

**Reconstitution Experiments.** Isolated  $F_1$  subunits, obtained by electroelution of SDS-PAGE bands of  $F_1$ , or the entire  $F_1$  sector at the concentrations described in the legend to the figures, were incubated 20 min with isolated  $F_0$  in 0.25 M sucrose, 10 mM Tris/acetate, pH 7.5, 1 mM EDTA, and 6 mM  $MgCl_2$ . The incubation was stopped by centrifugation at 105000g for 20 min.

**Preparation of  $F_0$  Vesicles.**  $F_0$  vesicles were prepared by the dialysis method (41). Three milligrams of  $F_0$  or  $F_0$  reconstituted with  $F_1$  or isolated  $F_1$  subunits was mixed with 30 mg of acetone-washed sonicated asolectin in 1 mL of 0.1 M potassium phosphate buffer, pH 7.2, containing 1.6% potassium cholate (w/v), 0.8% potassium deoxycholate (w/v), and 0.2 mM EDTA. The mixture was dialyzed overnight against 0.1 M potassium phosphate, pH 7.5, followed by a 3 h dialysis against 10 mM sodium tricine buffer, pH 7.5. Both dialysis media contained 0.25 mM EDTA and 2.5 mM  $MgSO_4$ .

**Measurement of Proton Conduction.** Proton conduction in submitochondrial particles was analyzed by following potentiometrically either the anaerobic release of the respiratory proton gradient (42) or proton release from submitochondrial particles or  $F_0$  liposomes induced by a diffusion potential (positive inside) imposed by valinomycin-mediated  $K^+$  influx (40). To minimize the electrode response time, a low-resistance and low-capacitance glass electrode connected to a MOS FET Electrometer amplifier, model 604 Keithley, was used. With this system pH changes in stirred suspensions can be measured with resolutions of 0.01 pH unit and overall rise time (10%–90% change) of less than 0.3–0.4 s (43). For the kinetic analysis of the proton release from submitochondrial particles or  $F_0$  liposomes, the potentiometric traces were converted into proton equivalents by double titration with standard HCl and KOH.

**Determination of P/O Ratios.** ATP produced by oxidative phosphorylation in ESMP or Mg-ATP particles was directly converted to glucose 6-phosphate with the addition of glucose and hexokinase in the reaction mixture (see legend to Table 4). The respiratory activity was measured following  $O_2$  uptake with a Clark oxygen electrode coated with a high-sensitivity membrane (YSI 5776) in a closed thermostatically controlled (25 °C) water-jacketed glass cell equipped with a magnetic stirrer. The  $O_2$  concentration of the reaction mixture was determined with NADH (44). Glucose-6-phosphate was determined on extracts of the particle suspension with glucose-6-phosphate dehydrogenase (45).

**Electrophoresis.** SDS-PAGE was performed on slab gels with a linear gradient of polyacrylamide (12%–20%) as in ref 22.

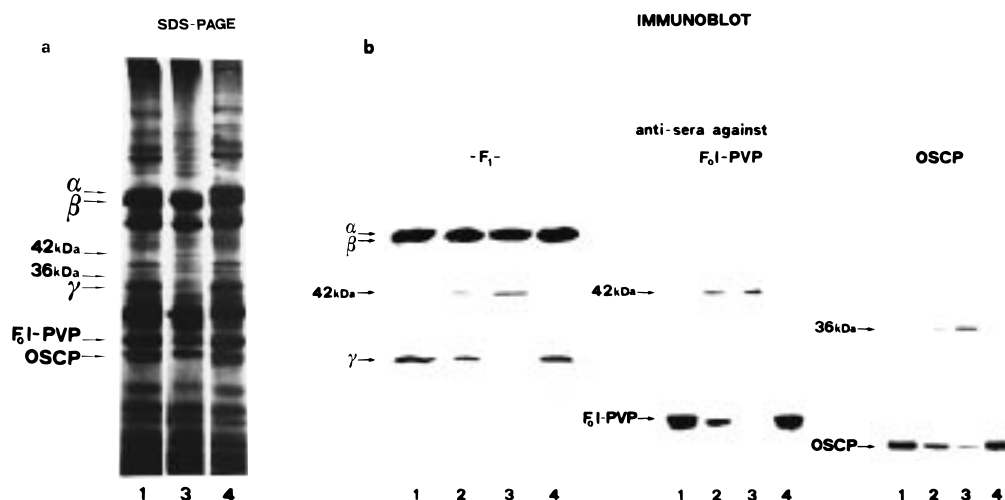


FIGURE 1: Coomassie blue stained SDS-PAGE slabs and immunoblot detection of cross-linking products of F<sub>1</sub>- $\gamma$ , F<sub>0</sub>I-PVP(b), and OSCP subunits in ESMP. ESMP were prepared as described under Materials and Methods: lane 1, control ESMP; lanes 2 and 3, ESMP incubated with 2 mM diamide for 2 and 5 min respectively; and lane 4, ESMP incubated 5 min with 2 mM diamide were then treated for 30 min with 20 mM DTT. For diamide treatment, ESMP were suspended in a reaction mixture containing the following: 200 mM sucrose, 30 mM KCl, and 20 mM K-succinate, pH 7.4. Incubation was carried out at 25 °C in a thermostatically controlled glass vessel under a constant stream of N<sub>2</sub>. Oxygen concentration was monitored polarographically. Once anaerobiosis was reached, 2 mM diamide was added and the incubation continued for 2 or 5 min. The reaction was stopped by the addition of 90% acetone (v/v). The washed pellets, obtained after centrifugation at 20000g, were solubilized in 2.3% SDS and 10 mM Tris-HCl, pH 6.8, and boiled for 3 min. (Panel a) Proteins (50  $\mu$ g) were applied on SDS slab gels with a linear gradient of polyacrylamide (12%–20%) and detected by Coomassie-blue staining. (Panel b) The proteins of the SDS-PAGE slabs were electrotransferred to nitrocellulose and immunodecorated with purified IgG fractions (46) of rabbit antisera raised against purified F<sub>1</sub>, F<sub>0</sub>I-PVP(b) and OSCP, respectively. For other details see under Materials and Methods.

**Immunological Procedures.** Polyclonal antibodies raised against SDS-denatured subunits F<sub>0</sub>I-PVP(b), OSCP, and  $\gamma$  were isolated from antisera collected after the 4<sup>th</sup>–6<sup>th</sup> booster injection in rabbits. The IgG fraction was purified by a combination of precipitations with caprylic acid and ammonium sulfate (46). The transfer of proteins from SDS-PAGE to nitrocellulose was performed in 125 mM Tris/HCl, pH 8.6, 192 mM glycine, 20% methanol (v/v) at about 100 mA for 1 h at room temperature in a semi-dry apparatus. After electrotransfer, the nitrocellulose sheets were blocked with 3% bovine serum albumin in 50 mM Tris/HCl, pH 7.4, 0.9% NaCl (w/v) for 1 h at 37 °C. Incubation with purified IgG fractions diluted in the same buffer was carried out overnight at 4 °C.

Immunoblotting was performed with a goat anti (rabbit IgG)-alkaline-phosphatase conjugate as indicator antibody for 1 h at room temperature (47). After each incubation step the excess protein was removed by extensive washing with 50 mM Tris/HCl, pH 7.4, 0.9% NaCl (w/v). Densitometric analysis of immunodecorated blots was performed with a Camag TLC Scanner II at 590 nm. The quantity of antigen detected was evaluated from the computed peak areas.

**Protein Determination.** Protein concentration was determined according to Lowry (48).

## RESULTS

Diamide, which oxidizes vicinal thiol groups followed by formation of disulfide bridges (49), induces in the mitochondrial F<sub>0</sub>F<sub>1</sub> complex cross-linking of F<sub>1</sub>- $\gamma$  and F<sub>0</sub>I-PVP(b) subunits, each one of them having a single cysteine residue (Cys197 in F<sub>0</sub>I-PVP(b) and Cys91 in F<sub>1</sub>- $\gamma$ ). Diamide treatment of submitochondrial particles (ESMP) caused, in fact, depending on the incubation time, partial or complete disappearance of the immunodetected bands of F<sub>1</sub>- $\gamma$  and F<sub>0</sub>I-PVP(b) subunits, from their original position in the SDS-

PAGE (Figures 1 and 3 and Table 1), and appearance in the gel of a new band (apparent Mw 42 kDa), which reacted with both anti-F<sub>1</sub> and anti F<sub>0</sub>I-PVP(b) antibodies and, upon reductive cleavage of disulfide bonds with DTT, disappeared with reappearance of these two protein bands in their original position (Figure 1 and Table 1). This cross-linking product of F<sub>1</sub>- $\gamma$  and F<sub>0</sub>I-PVP(b) was isolated from the gel, electrophoresed again, and immunodetected with both anti F<sub>1</sub> and anti F<sub>0</sub>I-PVP(b) antibodies (Figure 2). Upon reduction with DTT the isolated cross-linking product released the F<sub>1</sub>- $\gamma$  and F<sub>0</sub>I-PVP(b) subunits (Figure 2) (see also ref 28).

The diamide treatment of ESMP resulted also in disulfide cross-linking of OSCP (a single cysteine at position 118) with another thiol-bearing subunit (Figures 1 and 3 and Table 1). Its cross-linking product detected by the anti-OSCP antibody migrated in the SDS-PAGE with an apparent Mw of 36 kDa, different from that of the cross-linking product of F<sub>1</sub>- $\gamma$  and F<sub>0</sub>I-PVP(b) subunits, and did not cross-react with the polyclonal antibodies against these subunits. When a purified F<sub>0</sub> preparation was treated with diamide, the F<sub>0</sub>I-PVP(b) band was unaffected while that of OSCP was still decreased (Figures 3 and 4a) with the appearance of the cross-linking product which reacted with the antibody against OSCP but not with that against F<sub>0</sub>I-PVP(b) (Figure 4a). It should be noted that the purified F<sub>0</sub> preparation used did not contain any detectable trace of F<sub>1</sub>- $\gamma$  as shown by both Coomassie blue and silver staining (not shown) or immunodecoration with anti-F<sub>1</sub> antibody. The cross-linking product of OSCP obtained in the diamide-treated F<sub>0</sub> preparation was electroeluted from the gel and, upon reduction with DTT, released the OSCP subunit (Figure 4b).

When purified F<sub>0</sub> was reconstituted with purified F<sub>1</sub> or with the isolated F<sub>1</sub>- $\gamma$ , diamide treatment caused again, depending on the incubation time, partial or complete disappearance of the F<sub>0</sub>I-PVP(b) and of the F<sub>1</sub>- $\gamma$  band

Table 1: Diamide-Induced Disulfide Cross-Linking of F<sub>1</sub>- $\gamma$ , F<sub>0</sub>I-PVP(b), and OSCP in ESMP and Associated Effects on Anaerobic Relaxation of the Respiratory Proton Gradient

expts		control	control + DTT	1 <sup>st</sup> addition diamide	2 <sup>nd</sup> addition DTT
<b>A<sup>a</sup></b>	1/t <sub>1/2</sub> H <sup>+</sup> release (sec <sup>-1</sup> )	0.98	0.96	3.05	1.14
	immunoblot (arbitrary units) subunits: F <sub>1</sub> - $\gamma$	6.70	6.48	0.98	5.90
	F <sub>0</sub> I-PVP(b)	5.80	5.90	0.96	5.40
	OSCP	7.21	6.94	0.86	6.15
<b>B<sup>b</sup></b>	<sup>14</sup> [C]-DCCD (cpm) 8 kDa c subunit	2450		2600	

<sup>a</sup> ESMP (3 mg of protein/mL) were incubated in a medium containing the following: 200 mM sucrose, 30 mM KCl, and 20 mM succinate (potassium salt), pH 7.4. Incubation was carried out under a constant stream of N<sub>2</sub> at 25 °C. Once anaerobiosis was reached, 2 mM diamide was added and, after 2 min, the reaction was stopped by dilution with the same buffer and centrifugation at 105000g. Control and diamide-treated ESMP pellets were suspended in the same incubation mixture (3 mg of protein/mL) in the presence or in the absence of 20 mM DTT supplemented with 0.5  $\mu$ g of valinomycin/mg of ESMP protein and 13 000 units of catalase. Respiration-driven proton translocation was activated by repetitive pulses of 1%–3% H<sub>2</sub>O<sub>2</sub> (5  $\mu$ L/mL). The pH of the suspension was monitored potentiometrically as described under Materials and Methods. Then 50  $\mu$ g of protein was washed with 90% acetone (v/v) and centrifuged at 20000g, and the pellet, solubilized in 2.3% SDS and 10 mM Tris/HCl, pH 6.8, was boiled for 3 min. Proteins separated by PAGE were electrotransferred to nitrocellulose and immunodecorated with anti F<sub>0</sub>I-PVP(b), anti F<sub>1</sub>- $\gamma$ , and anti OSCP sera. Areas of  $\gamma$ , F<sub>0</sub>I-PVP(b), and OSCP immunoreactive bands were determined as arbitrary units by densitometric analysis of immunoblots, as reported under Materials and Methods. <sup>b</sup> ESMP and ESMP treated with diamide were incubated for 30 min with 50  $\mu$ M [<sup>14</sup>C]-DCCD in the same incubation mixture reported above (1 mg of protein/mL). The reaction was stopped by centrifugation at 105000g, and 300  $\mu$ g of particles was subjected to SDS–PAGE. After staining and destaining, a slice of the 8 kDa c subunit band was treated with Beckman tissue solubilizer 450 and the radioactivity determined by liquid scintillation counting.

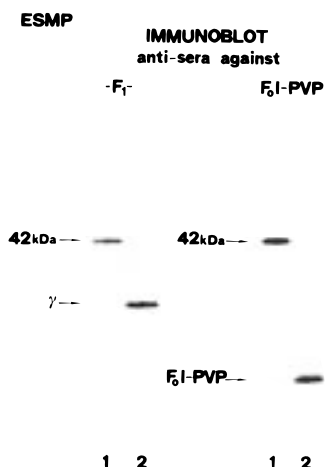


FIGURE 2: Immunodetection of the disulfide cross-linking product of F<sub>1</sub>- $\gamma$  and F<sub>0</sub>I-PVP(b) subunits induced by diamide treatment of ESMP. ESMP (300  $\mu$ g) treated with 2 mM diamide for 5 min, in the same experimental conditions reported in the legend to Figure 1, were subjected to SDS–PAGE. A piece of the gel slabs was cut between the  $\alpha/\beta$  and  $\gamma$  subunits, and proteins were electroeluted from it in buffered 50% glycerol as described in ref 40. Electroeluted proteins (lanes 1) and electroeluted proteins treated for 30 min at 25 °C with 20 mM DTT (lanes 2) were subjected to a second electrophoretic run followed by electrotransfer to nitrocellulose and immunodecoration with antisera against F<sub>1</sub> and F<sub>0</sub>I-PVP(b) subunits.

(Figure 3). It can be noted that the addition of F<sub>1</sub>- $\alpha/\beta$  to F<sub>0</sub> was, on the other hand, ineffective in this respect; furthermore the addition of F<sub>1</sub> or of its subunits had no effect on the diamide-induced decrease of the immunodetected band of OSCP (Figure 3). Diamide treatment of ESMP did not cause any cross-linking of F<sub>0</sub>-c subunits (a single cysteine at position 64), between them or another subunit, as shown by the fact that it did not decrease the amount of [<sup>14</sup>C]-DCCD-labeled original band of apparent Mr 8000 of this subunit (Table 1).

The results presented in Tables 1 and 2 show that diamide-induced cross-linking of F<sub>0</sub>I-PVP(b) and F<sub>1</sub>- $\gamma$  caused, both in ESMP (see also Figure 5) and in F<sub>0</sub> reconstituted with F<sub>1</sub> or with isolated F<sub>1</sub>- $\gamma$ , a dramatic enhancement of the oligomycin-sensitive proton conduction in F<sub>0</sub>. Diamide treatment of F<sub>0</sub>, which induced cross-linking of OSCP but left F<sub>0</sub>I-PVP(b) unaffected, had practically no effect on

oligomycin-sensitive proton conduction in F<sub>0</sub> liposomes (Table 2 and Figure 5). It should be noted that in the experiments presented in Figures 1–5 and Tables 1 and 2, submitochondrial particles (ESMP) and F<sub>0</sub> vesicles were treated with diamide in the absence of transmembrane  $\Delta\mu$ H<sup>+</sup> (28). Figure 5 shows that, when ESMP respiring with succinate as substrate were treated with diamide, no enhancement of the passive back-flow of protons took place. The immunoblot results presented in Figure 6 show that, under these conditions, diamide treatment of ESMP did not induce the cross-linking of F<sub>0</sub>I-PVP(b) with F<sub>1</sub>- $\gamma$  and of OSCP with another component of F<sub>0</sub>, as it did when ESMP were treated with diamide in anaerobiosis. Suppression of diamide-induced cross-linking of F<sub>1</sub> and F<sub>0</sub> subunits and the resulting enhancement of proton conduction is not merely due to the presence of oxygen, but this effect requires respiratory activity, as shown by the reappearance of F<sub>1</sub>- $\gamma$ , F<sub>0</sub>I-PVP(b), and OSCP cross-linking, upon inhibition of respiration by antimycin A (Figure 6). Suppression of diamide-induced cross-linking of F<sub>1</sub> and F<sub>0</sub> subunits was in fact dependent on the  $\Delta\mu$ H<sup>+</sup> generated by respiration and its dissipation through the proton channel in F<sub>0</sub>, as shown by restoration of cross-linking in respiring ESMP by FCCP (or nigericin), which abolishes the respiratory  $\Delta\mu$ H<sup>+</sup>, and by DCCD and oligomycin which inhibit proton conduction in F<sub>0</sub> (Table 3).

In another set of experiments the effect of diamide treatment of submitochondrial particles on proton pumping and ATP synthesis supported by succinate respiration was examined. Oxygen pulses of succinate supplemented ESMP or MgATP particles result in respiration-linked proton uptake. The efficiency of respiration-linked proton pumping can be evaluated from the extent of proton uptake at the respiring steady state and the H<sup>+</sup>/e<sup>-</sup> ratio, which is calculated from the ratio of the initial rate of proton release ensuing upon anaerobiosis and the steady-state respiratory rate measured just before anaerobiosis is reached (50). The results of these experiments are summarized in Table 4. Treatment of ESMP or MgATP-SMP with diamide, both in the respiring state (non cross-linking conditions) and in anaerobiosis (cross-linking conditions), had no effect on the rate of succinate respiration and the extent of respiratory proton uptake.

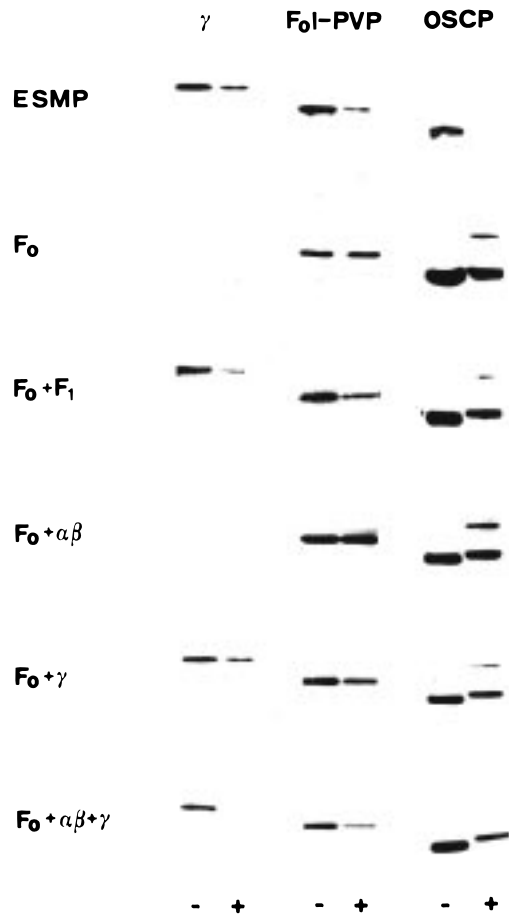


FIGURE 3: Immunoblot analysis of disulfide cross-linking of ATP synthase subunits in ESMP and in  $F_0$  liposomes. ESMP,  $F_1$ ,  $F_1$  subunits, and  $F_0$  sector were prepared as described under Materials and Methods. Where indicated, isolated subunits or  $F_1$  was added to  $F_0$  at the concentration of 4  $\mu\text{g}/\text{mg}$  or 0.5  $\text{mg}/\text{mg}$  of protein  $F_0$ , respectively. The incubation was stopped by centrifugation at 105000g to eliminate the excess of  $F_1$  or  $F_1$  subunits. The binding to  $F_0$  of added  $\alpha\beta$  and  $\gamma$  subunits was directly verified by immunoblots of the precipitated pellet.  $F_0$  and  $F_0$  reconstituted with  $F_1$  or  $F_1$  subunits were incorporated in liposomes by the dialysis method described under Materials and Methods. ESMP and  $F_0$  liposomes were treated with diamide in the succinate mixture described in the legend to Figure 1, after the suspension was made anaerobic by respiratory activity under a constant stream of  $\text{N}_2$  at 25  $^\circ\text{C}$ . Once anaerobiosis was reached, 2 mM diamide was added and the incubation continued for 2 min. The reaction was stopped by the addition of 90% acetone (v/v). The washed pellets, obtained after centrifugation at 20000g, were solubilized in 2.3% SDS and 10 mM Tris/HCl, pH 6.8, and boiled for 3 min. Proteins (50  $\mu\text{g}$ ) were subjected to gel electrophoresis, electrotransferred to nitrocellulose, and immunodecorated with anti- $F_1$ , anti-FoI-PVP(b), and anti-OSCP sera. For other details see under Materials and Methods.

Treatment of ESMP with diamide in anaerobiosis resulted in an increase of the rate of proton back-flow and enhancement of the steady-state  $\text{H}^+/\text{e}^-$  ratio for proton pumping from 1.2 to 3.0, which is the upper limit for proton pumping with succinate as respiratory substrate (51). The remarkable enhancement of the  $\text{H}^+/\text{e}^-$  ratio is consistent with the increase in the rate of proton back-flow through  $F_0$ , which prevents decoupling of redox-driven proton pump by transmembrane  $\Delta\text{pH}$  (51–53). This finding suggests, incidentally, that the entry mouth of the proton channel of the  $F_0F_1$  complex in the membrane can get very close to the output mouth of the proton pumps in respiratory complexes so as to drain effectively, under the prevailing experimental conditions

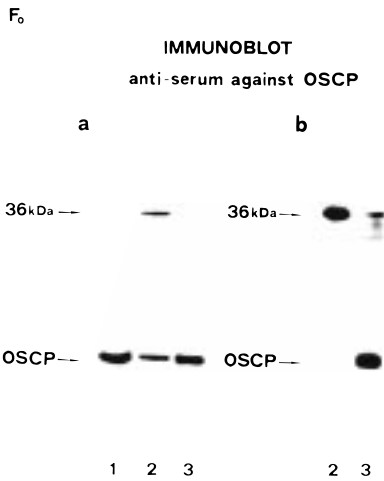


FIGURE 4: Immunodecoration of the cross-linking product of OSCP subunit induced by diamide treatment of  $F_0$  liposomes. Purified  $F_0$  was prepared as described under Materials and Methods.  $F_0$  was incorporated in liposomes by the dialysis method described under Materials and Methods.  $F_0$  liposomes were treated for 5 min with 2 mM diamide in the succinate mixture as described in the legend to Figure 1. The reaction was stopped by the addition of 90% acetone (v/v). After centrifugation at 20000g, the washed pellet was solubilized in 2.3% SDS and 10 mM Tris-HCl, pH 6.8, and boiled for 3 min. (Panel a) Proteins (50  $\mu\text{g}$ ) were subjected to gel electrophoresis, electrotransferred to nitrocellulose, and immunodecorated with anti-OSCP serum: lane 1, control; lane 2,  $F_0$  liposomes treated with diamide; lane 3, diamide-treated  $F_0$  liposomes incubated 30 min with 20 mM DTT. (Panel b)  $F_0$  liposomes (200  $\mu\text{g}$ ), treated with diamide, were subjected to SDS-PAGE. A piece of the gel slab was cut between the  $\alpha\beta$  and  $\gamma$  subunits, and the proteins were electroeluted as described in the legend to Figure 2. Electroeluted proteins (lane 2) and electroeluted proteins treated 30 min with 20 mM DTT (lane 3) were subjected to a second electrophoretic run followed by electrotransfer to nitrocellulose and immunodecoration with anti-OSCP serum.

Table 2: Effect of Diamide-Induced Disulfide Cross-Linking of  $F_0$  and  $F_1$  Subunits on Proton Conduction in ESMP and  $F_0$  Liposomes

additions	$\text{H}^+$ release ( $\text{nmol} \cdot \text{min}^{-1} \cdot \text{mg}$ of protein $^{-1}$ )			
	without oligomycin		with oligomycin	
	– diamide	+ diamide	– diamide	+ diamide
ESMP	174.4	610.0	31.4	98.3
$F_0$ liposomes	760.1	625.1	112.4	78.4
+ $F_1$	484.1	1348.9	50.3	104.3
+ $\alpha\beta$	706.9	582.0	101.3	74.3
+ $\gamma$	440.3	1423.1	52.7	112.9
+ $\alpha\beta + \gamma$	408.4	795.3	52.3	96.4

<sup>a</sup> Preparation of ESMP,  $F_1$ ,  $F_0$ , and  $F_1$  subunits, reconstitution procedures, diamide treatment, and incorporation into liposome vesicles were carried out as described under Materials and Methods and in the legend to Figure 3. For measurement of  $\text{H}^+$  conduction, ESMP (1  $\text{mg}$  of protein/mL) and  $F_0$  liposomes (0.4  $\text{mg}$  of protein/mL) were suspended in 0.15 M KCl, and passive  $\text{H}^+$  release induced by  $\text{K}^+$  uptake was initiated by the addition of valinomycin (2  $\mu\text{g}/\text{mg}$  of particles protein). Where indicated, submitochondrial particles and  $F_0$  liposomes were incubated for 5 min with 1.0  $\mu\text{g}$  of oligomycin/mg of particles protein before the addition of 0.15 M KCl and valinomycin. For other details see under Materials and Methods.

used, the respiratory  $\Delta\mu\text{H}^+$ . Although the coupling efficiency of redox-linked proton pumping was, under these conditions, increased, the coupling efficiency for the utilization of respiratory  $\Delta\mu\text{H}^+$  by the  $F_0F_1$  complex to synthesize ATP was decreased by the  $F_1$ - $\gamma$  and  $F_0$ I-PVP(b) cross-linking induced by diamide, as shown by the decrease of the P/O ratio. Internal control experiments show, clearly, that

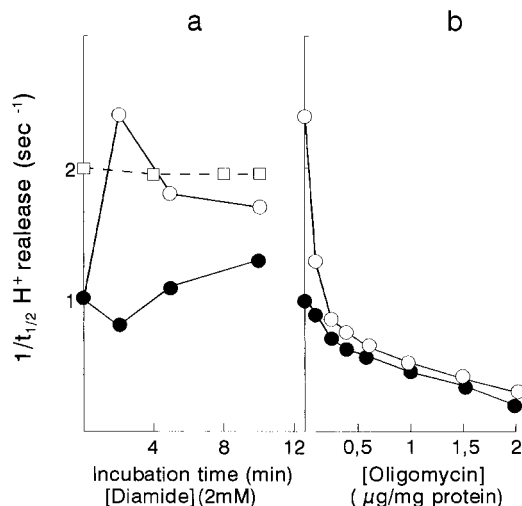


FIGURE 5: Effect on proton conduction of diamide treatment of ESMP and  $F_0$  liposomes. (Panel a) ESMP were treated with diamide for the times indicated in the figure in the succinate mixture described in the legend to Table 1 after the suspension was made anaerobic by respiratory activity under a constant stream of  $N_2$  at 25 °C (○). ESMP, respiring with succinate in the mixture described in the legend to Table 1, were incubated with diamide (●). At the time indicated in the figure the reaction was stopped by dilution with the same standard medium and the suspension centrifuged at 105000g. In both cases the ESMP pellet was suspended in the succinate reaction mixture containing valinomycin and catalase (see legend to Table 1) and respiration-driven proton translocation was activated by repetitive pulses of  $H_2O_2$ .  $F_0$  liposomes were treated with diamide and suspended in 0.15 M KCl (□);  $H^+$  release was initiated by the addition of 2  $\mu$ g of valinomycin/mg of  $F_0$ . (Panel b) Before starting respiration with  $H_2O_2$  pulses in the presence of catalase, ESMP (●) and ESMP treated for 2 min in anaerobiosis with 2 mM diamide (○) were incubated for 2 min with oligomycin at the concentrations reported in the figure. For other details see the legend to Table 1 and under Materials and Methods.

diamide was without any of these effects when added to respiring ESMP, conditions in which cross-linking of  $F_0F_1$  subunits is prevented. The effects produced by the anaerobic treatment of ESMP with diamide are also observed in MgATP particles. In these particles, which retain a better capacity for oxidative phosphorylation, as compared to ESMP, anaerobic treatment with diamide caused a more definite decrease of the P/O ratio, although the enhancing effect of diamide treatment on the rate of proton back-flow and on the  $H^+/e^-$  ratio for proton pumping was smaller, probably due to the preservation of a tighter native asset of the  $F_0F_1$  complex in these particles.

## DISCUSSION

The  $F_0I$ -PVP(b) subunit, present in one copy in the mitochondrial  $F_0F_1$ -ATP synthase (54), (in the *E. coli* enzyme there are two copies of the corresponding b subunit (11)), is essential for the binding of the  $F_1$  head piece to the  $F_0$  membrane sector (16–18, 22, 23, 31). The carboxy-terminal region of  $F_0I$ -PVP(b) protrudes out of the membrane integral part of  $F_0$ , where it is anchored, at the lateral side of the bundle of c subunits, by two hydrophobic helices of the N-terminal region, and reaches the surface of the  $F_1$  complex (4, 17, 31, 54). OSCP in the mitochondrial (54) and the homologous  $F_1\delta$  in the *E. coli* ATP synthase (55) apparently extend from the stalk, where they interact with the C-terminal region of the b subunit, all along the surface of  $F_1$ . The

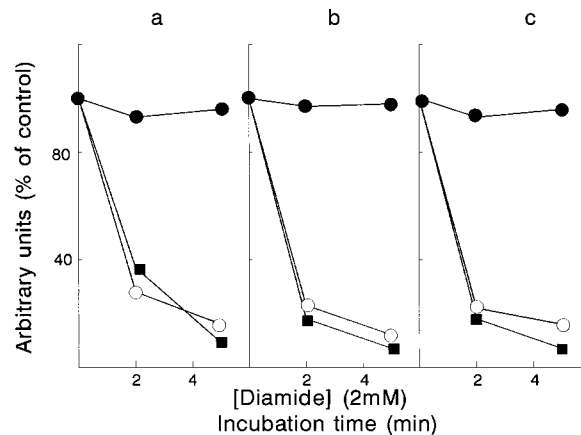


FIGURE 6: Effect of respiration on diamide-induced disulfide cross-linking of  $F_1\gamma$ ,  $F_0I$ -PVP(b), and OSCP in ESMP. ESMP (3 mg of protein/mL) were incubated with 2 mM diamide in the succinate mixture reported in the legend to Table 1 for the time given in the figure in anaerobiosis (○), in succinate-respiring state (see legend to Figure 2) (●), and in aerobiosis in the presence of 1.0  $\mu$ g of antimycin A/mg of particle protein to inhibit succinate-supported respiration (■). A 50  $\mu$ g protein sample of ESMP was treated as described in the legend to Figure 1 for densitometric analysis of immunodecorated bands of  $F_0I$ -PVP(b) (a),  $F_1\gamma$  (b), and OSCP (c). The percentage of antigen detected in the bands was evaluated from the computed peak areas taking as 100% the peak areas in untreated ESMP. For other details see the legend to Table 1 and under Materials and Methods.

$F_1\gamma$  subunit, which penetrates with its C and N termini the central cavity of the  $\alpha\beta\beta_3$  hexamer of  $F_1$ , constitutes with its large central lobe, of which a short lateral  $\alpha$ -helix (residues 73–90) is identified in the  $F_1$  crystal (5), a large part of the stalk.

It has been proposed that the two b subunits in *E. coli* and the single copy of  $F_0I$ -PVP(b) subunit in the mitochondrial enzyme, together with  $F_1\delta$  in *E. coli*, and the corresponding OSCP in mitochondria, constitute a stator attached to the surface of the  $\alpha\beta\beta_3$  hexamer while the  $\gamma$  and  $\epsilon$  subunits, in *E. coli*, and  $\gamma$  and  $\delta$  in mitochondria represent, together with the bundle of c subunits, the rotor of the ATP synthase rotary motor (3, 8, 33, 55). According to the rotatory model, proton flow through a channel at the interface of subunit a and c subunits generates a torque which drives the rotor and stator in the opposite direction (33, 56). Our finding that cross-linking of the  $F_1\gamma$  and  $F_0I$ -PVP(b), through disulfide cross-linking of Cys 91 of  $\gamma$  and Cys 197 in  $F_0I$ -PVP(b), and hence their relative immobilization results in opening of the matrix mouth of the proton channel of  $F_0$  with rapid dissipative diffusion through it of the respiratory proton gradient “decoupled” from ATP synthesis, is consistent with and provides support to the view that the  $F_0I$ -PVP(b) and  $F_1\gamma$  are components of the stator and rotor element, respectively.

It seems worth noting here that Cys91 of the mitochondrial  $F_1\gamma$  is conserved in the chloroplast  $F_1\gamma$  subunit (Cys89), which has, in addition 3 other cysteines (Cys199, Cys205, Cys322) (57). It has been found that internal cross-linking of Cys89 with one of the other three cysteine residues in the chloroplast  $F_1\gamma$  caused a pronounced increase in proton conduction (58).

One important aspect of the rotary motor of ATP synthase is represented by the topological organization of the stator and the rotor in the stalk. Contrary to a general view of the

Table 3: Effect of FCCP, DCCD, Nigericin, and Oligomycin on Diamide-Induced Disulfide Cross-Linking of F<sub>1</sub>- $\gamma$ , F<sub>0</sub>I-PVP(b), and OSCP in Respiring ESMP<sup>a</sup>

additions	immunoblot (% of control)					
	anti $\gamma$ serum		anti F <sub>0</sub> I-PVP(b) serum		anti OSCP serum	
	– diamide	+ diamide	– diamide	+ diamide	– diamide	+ diamide
ESMP-AS <sup>b</sup>	100	29	100	24	100	23
ESMP-RS <sup>c</sup>	100	94	100	97	100	94
ESMP-RS + FCCP	97	30	99	27	96	20
ESMP-RS + DCCD	98	28	98	24	98	18
ESMP-RS + nigericin	99	26	97	20	99	24
ESMP-RS + oligomycin	100	28	100	27	100	22

<sup>a</sup> ESMP (3 mg of protein/mL) were incubated in anaerobiosis or in the succinate respiring state in the experimental conditions given in the legend to Figure 5. Where indicated 1  $\mu$ M FCCP, 0.5 mM DCCD, 0.5  $\mu$ g of nigericin/mg of particles protein, or 1  $\mu$ g of oligomycin/mg particles protein were added. The incubation time was 2 min, except with DCCD which was 30 min. ESMP were then incubated with 2 mM diamide for 2 min and treated for immunodecoration with antibodies. Immunodecoration of SDS–PAGE of ESMP with antibodies and densitometric analysis was carried out as described in the legend to Table 1 and under Materials and Methods. The percentage of antigen detected in the bands was evaluated from the computed peak areas taking as 100% the peak areas in diamide-untreated ESMP. For other details see legend to Table 1 and under Materials and Methods. <sup>b</sup> ESMP-AS: submitochondrial particles incubated in anaerobiosis. <sup>c</sup> ESMP-RS: submitochondrial particles incubated in the succinate-respiring state.

Table 4: Effect of Diamide on H<sup>+</sup>/e<sup>–</sup> Ratio and P/O in Anaerobiosis and in the Succinate-Respiring State in ESMP and in MgATP-SMP<sup>a</sup>

	respiration rate ng O/(min mg)	extent H <sup>+</sup> uptake ng of H <sup>+</sup> /mg	V H <sup>+</sup> ng of H <sup>+</sup> /(mg min)	H <sup>+</sup> /e <sup>–</sup>	ATP synthesis nmol of ATP/(mg min)	P/O
ESMP	115 $\pm$ 9.6	2.8 $\pm$ 0.1	69.5 $\pm$ 5.8	1.22 $\pm$ 0.20	29.3 $\pm$ 2.3	0.26 $\pm$ 0.04
ESMP-AS + diamide <sup>b</sup>	129 $\pm$ 12.9	3.0 $\pm$ 0.1	195.0 $\pm$ 19.5	3.09 $\pm$ 0.61	20.6 $\pm$ 1.3	0.16 $\pm$ 0.02
ESMP-SRS + diamide <sup>c</sup>	114 $\pm$ 8.8	2.7 $\pm$ 0.2	71.9 $\pm$ 5.5	1.27 $\pm$ 0.19	30.3 $\pm$ 1.1	0.27 $\pm$ 0.03
MgATP-SMP	103 $\pm$ 7.8	2.7 $\pm$ 0.1	34.0 $\pm$ 2.6	0.67 $\pm$ 0.10	71.4 $\pm$ 4.1	0.70 $\pm$ 0.09
MgATP-AS + diamide <sup>d</sup>	114 $\pm$ 8.3	2.8 $\pm$ 0.1	46.8 $\pm$ 3.4	0.83 $\pm$ 0.12	25.6 $\pm$ 3.2	0.23 $\pm$ 0.04
MgATP-SRS + diamide <sup>e</sup>	95 $\pm$ 5.9	2.7 $\pm$ 0.1	30.3 $\pm$ 1.9	0.64 $\pm$ 0.08	63.2 $\pm$ 3.8	0.67 $\pm$ 0.08

<sup>a</sup> ESMP (3 mg of protein/mL) or MgATP-SMP (3 mg of protein/mL) was incubated in the succinate reaction mixture described in the legend to Figure 1, in the thermostatically controlled glass cell at 25 °C, kept for the respiring state open and under a gentle stream of N<sub>2</sub> for the anaerobic treatment. Anaerobic or respiring particles were incubated for 2 min with 2 mM diamide. To measure respiration-driven proton uptake and the following anaerobic relaxation of the respiratory proton gradient, we supplemented the particles suspension, kept in the closed glass cell, with valinomycin and catalase and activated respiration with pulses of 1%–3% H<sub>2</sub>O<sub>2</sub> (5  $\mu$ L/mL) as described in the legend to Table 1. To measure P/O ratios of oxidative phosphorylation, we incubated the particles (1 mg of protein/mL) in a mixture containing the following: 200 mM sucrose, 10 mM K-succinate, 3 mM MgCl<sub>2</sub>, 1 mM EDTA, 10 mM potassium phosphate, pH 7.4, 20 mM glucose, 5 units hexokinase, and 300  $\mu$ M p<sub>i</sub>, p<sub>5</sub> Di (Adenosin-5-) pentaphosphate (to inhibit adenylate kinase). MgADP (300  $\mu$ M) was added, and the respiratory rate in state 3 was measured for 5 min. To measure the ATP synthesized in this interval, 500  $\mu$ L of the submitochondrial particles suspension was treated with 500  $\mu$ L of 28% perchloric acid (w/v). After centrifugation at 20000g, the supernatant was cooled in ice and neutralized with 60% KOH (w/v), then cleared by centrifugation. The neutralized suspension (700  $\mu$ L) was added to a mixture containing the following: 1 mM MgCl<sub>2</sub>, 150 mM Tris/HCl, pH 7.4, and 7 units glucose-6 phosphate dehydrogenase. NADP (1 mM) was added and glucose-6-phosphate was determined following spectrophotometric NADP reduction at 340 nm. The values reported in the Table are the means of 4 experiments  $\pm$  S.E.M. <sup>b</sup> ESMP-AS: submitochondrial particles incubated in anaerobiosis. <sup>c</sup> ESMP-RS: submitochondrial particles incubated in the succinate-respiring state. <sup>d</sup> MgATP-SMP-AS: submitochondrial particles incubated in anaerobiosis. <sup>e</sup> MgATP-SMP-RS: submitochondrial particles incubated in the succinate-respiring state.

structure of the F<sub>0</sub>F<sub>1</sub>-ATP synthase, based on electron microscopy studies (1, 13, 59–61) according to which the F<sub>0</sub>I-PVP(b),  $\gamma$ , OSCP ( $\delta$  in *E. coli*),  $\delta$  ( $\epsilon$  in *E. coli*) and other mitochondrial supernumerary subunits are assembled in a single stalk, it has recently been proposed, on the basis of cross-linking data in the *E. coli* F<sub>0</sub>F<sub>1</sub> complex, that the b and  $\delta$  subunit of the proposed stator in *E. coli* (F<sub>0</sub>I-PVP(b) and OSCP in mitochondria) constitute a second lateral stalk separate from the  $\gamma$  and  $\epsilon$  ( $\delta$  in mitochondria) rotor which constitute the central stalk (3, 33, 55). Recent average analysis of electron microscopy images of *E. coli* F<sub>0</sub>F<sub>1</sub>-ATP synthase shows, in addition to the fatter central stalk, a lateral thin structure which is considered to represent a second stalk made up by the F<sub>0</sub>-b and F<sub>1</sub>- $\delta$  subunits (62).

The present finding that, in the absence of a respiratory  $\Delta\mu$ H<sup>+</sup>, diamide induces disulfide bridging of Cys 197 in the carboxyl-terminal region of F<sub>0</sub>I-PVP(b) with Cys 91 at the C-terminus of the lateral short  $\alpha$ -helix (residues 73–90) of  $\gamma$  shows that these two domains, at least in the resting enzyme in the absence of a transmembrane  $\Delta\mu$ H<sup>+</sup>, are in direct contact rather than being separated as it would be

suggested by the recent electron microscopy images of the *E. coli* F<sub>0</sub>F<sub>1</sub>-ATPase (62). The prevention of diamide-induced disulfide cross-linking of F<sub>0</sub>I-PVP(b) and  $\gamma$  subunit, when the  $\Delta\mu$ H<sup>+</sup> generated by respiration relaxes through the F<sub>0</sub> channel, provides evidence showing that the torque generated by the proton flow generates a relative motion and/or a separation of these two subunits which places the two cysteine residues at a distance at which they can no longer be engaged in disulfide bridging.

In the resting enzyme diamide also induces disulfide cross-linking of OSCP with another component of F<sub>0</sub>. This is not subunit c as shown by the lack of diamide effect on the level of the [<sup>14</sup>C]-DCCD label of the band of Mr 8000 of this subunit. The two possible candidates are subunits d or f of F<sub>0</sub>, both of which have a single cysteine residue. Cross-linking of OSCP with either of these two subunits, which is also prevented by proton flow through F<sub>0</sub>, has no significant effect on proton conduction in F<sub>0</sub> as, in fact, expected when cross-linking occurs between two components of the stator element of the rotary motor.

## REFERENCES

1. Gogol, E. P., Lucken, U., and Capaldi, R. A. (1987) *FEBS Lett.* 219, 274–278.
2. Cox, G. B., Devenish, R. J., Gibson, F., Howitt, S. M., and Nagley, P. (1992) *Molecular Mechanism in Bioenergetics* (Ernster, L., Ed.) pp 283–315, Elsevier, Amsterdam, The Netherlands.
3. Ogilvie, I., Aggeler, R., and Capaldi, R. A. (1997) *J. Biol. Chem.* 272, 16652–16656.
4. Papa, S., Xu, T., Gaballo, A., and Zanotti, F. (1998) in *Frontiers of Cellular Bioenergetics: Molecular Biology, Biochemistry and Physiopathology* (Papa, S., Guerrieri, F., and Tager, J. M., Eds.) Plenum Press, London, New York (in press).
5. Abrahams, J. P., Leslie, A. G. W., Lutter, R., and Walker, J. E. (1994) *Nature* 370, 621–628.
6. Boyer, P. D. (1997) *Annu. Rev. Biochem.* 66, 717–749.
7. Duncan, T. M., Bulygin, V. V., Zhou, Y., Hutcheon, M. L., and Cross, R. L. (1995) *Proc. Natl. Acad. Sci. U.S.A.* 92, 10964–10968.
8. Sabbert, D., Engelbrecht, S., and Junge, W. (1996) *Nature* 381, 623–625.
9. Noji, H., Yasuda, R., Yoshida, M., and Kinoshita, K. (1997) *Nature* 386, 299–302.
10. Schneider, E., and Altendorf, K. (1987) *Microbiol. Rev.* 51, 477–497.
11. Fillingame, R. H. (1996) *Curr. Opin. Struct. Biol.* 6, 491–498.
12. Howitt, S. M., Rodgers, A. J. W., Hatch, L. P., Gibson, F., and Cox, G. B. (1996) *J. Bioenerg. Biomembr.* 28, 415–420.
13. Capaldi, R. A., Aggeler, R., Turina, P., and Wilkens, S. (1994) *Trends Biochem. Sci.* 19, 284–289.
14. Wilkens, S., Dahlquist, F. W., McIntosh, L. P., Donaldson, L. W., and Capaldi, R. A. (1995) *Nat. Struct. Biol.* 2, 961–967.
15. Schneider, E., and Altendorf, K. (1985) *Eur. J. Biochem.* 153, 105–109.
16. Houstek, J., Kopecky, J., Zanotti, F., Guerrieri, F., Jirillo, E., Capozza, G., and Papa, S. (1988) *Eur. J. Biochem.* 173, 1–8.
17. Papa, S., Guerrieri, F., Zanotti, F., Houstek, J., Capozza, G., and Ronchi, S. (1989) *FEBS Lett.* 249, 62–66.
18. Walker, J. E., Lutter, R., Dupuis, A., and Runswick, M. J. (1991) *Biochemistry* 30, 5369–5378.
19. Herrmann, R. G., Steppuhn, J., Herrmann, G. S., and Nelson, N. (1993) *FEBS Lett.* 326, 192–198.
20. Collinson, I. R., Runswick, M. J., Buchanan, S. K., Fearnley, I. M., Skehel, J. M., van Raaij, M. J., Griffiths, D. E., and Walker, J. E. (1994) *Biochemistry* 33, 7971–7978.
21. Belogradov, G. I., Tomich, J. M., and Hatefi, Y. (1996) *J. Biol. Chem.* 271, 20340–20345.
22. Zanotti, F., Guerrieri, F., Capozza, G., Houstek, J., Ronchi, S., and Papa, S. (1988) *FEBS Lett.* 237, 9–14.
23. Heckman, C., Tomich, J. M., and Hatefi, Y. (1991) *J. Biol. Chem.* 266, 13564–13571.
24. Collinson, I. R., Fearnley, I. M., Skehel, J. M., Runswick, M. J., and Walker, J. E. (1994) *Biochem. J.* 303, 639–645.
25. Papa, S., Guerrieri, F., Zanotti, F., Fiermonte, M., Capozza, G., and Jirillo, E. (1990) *FEBS Lett.* 272, 117–120.
26. Dupuis, A., Issartel, J. P., Lunardi, J., Satre, M., and Vignais, P. V. (1985) *Biochemistry* 24, 728–733.
27. Archinard, P., Godinot, C., Comte, J., and Gautheron, D. C. (1986) *Biochemistry* 25, 3397–3404.
28. Zanotti, F., Guerrieri, F., Capozza, G., Fiermonte, M., Berden, J., and Papa, S. (1992) *Eur. J. Biochem.* 208, 9–16.
29. Belogradov, G. I., Tomich, J. M., and Hatefi, Y. (1995) *J. Biol. Chem.* 270, 2053–2060.
30. Watts, S. D., Zhang, Y., Fillingame, R. H., and Capaldi, R. A. (1995) *FEBS Lett.* 368, 235–238.
31. Collinson, I. R., van Raaij, M. J., Runswick, M. J., Fearnley, I. M., Skehel, J. M., Orriss, G. L., Miroux, B., and Walker, J. E. (1994) *J. Mol. Biol.* 242, 408–421.
32. Zhou, Y., Duncan, T. M., and Cross, R. L. (1997) *Proc. Natl. Sci. U.S.A.* 94, 10583–10587.
33. Junge, W., Lill, M., and Engelbrecht, S. (1997) *Trends Biochem. Sci.* 22, 420–423.
34. Low, H., and Vallin, J. (1963) *Biochim. Biophys. Acta* 69, 361–374.
35. Lee, C. P., and Ernster, L. (1968) *Eur. J. Biochem.* 3, 391–400.
36. Racker, E., and Hostman, L. L. (1967) *J. Biol. Chem.* 242, 2547–2551.
37. Guerrieri, F., and Papa, S. (1981) *J. Bioenerg. Biomembr.* 13, 393–400.
38. Guerrieri, F., Capozza, G., Houstek, J., Zanotti, F., Colaianni, G., Jirillo, E., and Papa, S. (1989) *FEBS Lett.* 250, 60–66.
39. Beechey, R. B., Hubbard, S. A., Linnett, P. E., Mitchell, A. D., and Munn, E. A. (1975) *Eur. J. Biochem.* 242, 2547–2551.
40. Zanotti, F., Guerrieri, F., Che, Y. W., Scarfò, R., and Papa, S. (1987) *Eur. J. Biochem.* 164, 517–523.
41. Okamoto, M., Sone, H., Hirata, H., Yoshida, H., and Kagawa, Y. (1977) *J. Biol. Chem.* 252, 6125–6131.
42. Pansini, A., Guerrieri, F., and Papa, S. (1978) *Eur. J. Biochem.* 92, 545–551.
43. Papa, S., Guerrieri, F., and Rossi Bernardi, L. (1978) *Methods in Enzymology* LV, 614–627.
44. Estabrook, R. W. (1967) *Methods in Enzymology* X, 41–47.
45. Papa, S., Tager, J. M., Guerrieri, F., and Quagliariello, E. (1969) *Biochim. Biophys. Acta* 172, 184–186.
46. McKinney, M. M., and Parkinson, A. (1987) *J. Immunol. Methods* 96, 271–278.
47. Hensel, M., Deckers-Hebestreit, G., Schmid, R., and Altendorf, K. (1990) *Biochim. Biophys. Acta* 1016, 63–70.
48. Lowry, O. H., Rosebrough, N. J., Farr, A. L., and Randall, R. J. (1951) *J. Biol. Chem.* 193, 265–275.
49. Kosower, E. M., Corea, W., Kinon, B. J., and Kosower, W. S. (1972) *Biochim. Biophys. Acta* 264, 39–44.
50. Papa, S., Guerrieri, F., Simone, S., Lorusso, M., and Larosa, D. (1973) *Biochim. Biophys. Acta* 292, 20–38.
51. Papa, S., Lorusso, M., and Capitanio, N. (1994) *J. Bioenerg. Biomembr.* 26, 609–618.
52. Cocco, T., Lorusso, M., Di Paola, M., Minuto, M., and Papa, S. (1992) *Eur. J. Biochem.* 209, 475–481.
53. Capitanio, N., Capitanio, G., Demarinis, D. A., De Nitto, E., Massari, S., and Papa, S. (1996) *Biochemistry* 35, 10800–10806.
54. Collinson, I. R., Skehel, J. M., Fearnley, I. M., Runswick, M. J., and Walker, J. E. (1996) *Biochemistry* 35, 12640–12646.
55. Wilkens, S., Dunn, S. D., Chandler, J., Dahlquist, F. W., and Capaldi, R. A. (1997) *Nat. Struct. Biol.* 4, 198–201.
56. Elston, T., Wang, H., and Oster, G. (1998) *Nature* 391, 510–513.
57. McCarty, R. E., and Nalin, C. M. (1986) *Plant Physiol.* 19, 576–583.
58. Moroney, J. V., and McCarty, R. E. (1979) *J. Biol. Chem.* 254, 8951–8955.
59. Fernandez-Moran, H. (1962) *Circulation* 26, 1039–1065.
60. Lucken, U., Gogol, E. P., and Capaldi, R. A. (1990) *Biochemistry* 29, 5339–5343.
61. Walker, J. E., and Collinson, I. R. (1994) *FEBS Lett.* 346, 39–43.
62. Wilkens, S., and Capaldi, R. A. (1998) *Nature* 393, 29.

BI981422C